

Deforming nanocrystalline nickel at ultrahigh strain rates

Y. M. Wang,^{a)} E. M. Bringa, J. M. McNaney, M. Victoria, A. Caro, A. M. Hodge, R. Smith, B. Torralva, and B. A. Remington

Lawrence Livermore National Laboratory, Livermore, California 94550

C. A. Schuh

Department of Materials Science and Engineering, Massachusetts Institute of Technology, Cambridge, Massachusetts 02139

H. Jamarkani and M. A. Meyers

Department of Mechanical and Aerospace Engineering, University of California, San Diego, California 92093

(Received 23 November 2005; accepted 19 January 2006; published online 10 February 2006)

The deformation mechanism of nanocrystalline Ni (with grain sizes in the range of 30–100 nm) at ultrahigh strain rates ($>10^7 \text{ s}^{-1}$) was investigated. A laser-driven compression process was applied to achieve high pressures (20–70 GPa) on nanosecond timescales and thus induce high-strain-rate deformation in the nanocrystalline Ni. Postmortem transmission electron microscopy examinations revealed that the nanocrystalline structures survive the shock deformation, and that dislocation activity is a prevalent deformation mechanism for the grain sizes studied. No deformation twinning was observed even at stresses more than twice the threshold for twin formation in micron-sized polycrystals. These results agree qualitatively with molecular dynamics simulations and suggest that twinning is a difficult event in nanocrystalline Ni under shock-loading conditions. © 2006 American Institute of Physics. [DOI: 10.1063/1.2173257]

The current understanding of atomic-scale deformation mechanisms in nanocrystalline (nc) metals relies heavily on molecular dynamics (MD) simulations. Due to the short time and length scales necessitated by these simulations, they are generally conducted at strain rates $>10^7 \text{ s}^{-1}$ ^{1–3} much higher than typical experimental ones ($<10^4 \text{ s}^{-1}$).^{4,5} Such ultrahigh strain rate deformation can be experimentally realized through high-pressure shocks, but has never been applied to nanocrystalline materials before. Recent atomistic simulations⁶ indicate that, under shock-loading conditions, the flow stress of nc Cu reaches extremely high values due to kinetic limitations on grain-boundary sliding. Shock-loading provides not only very high deformation rates ($>10^7 \text{ s}^{-1}$), but also a unique combination of high hydrostatic pressure and shear stress in the shocked material. It is speculated that other deformation mechanisms may arise in nc materials under such extreme deformation conditions. The purpose of this letter is to investigate these deformation mechanisms using a model material, nanocrystalline nickel (with grain sizes of 30–100 nm), subjected to shock pressures of 20–70 GPa.

There are a number of shock experiments reported for coarse-grained polycrystalline Ni with grain sizes down to 25 μm .^{7–9} Recovered shock-loaded samples exhibit dislocation cells at pressures below 30 GPa, with stacking faults and twins forming above this threshold pressure;⁹ these microstructural features have been found to harden the recovered materials. We are not aware of similar experiments on nc samples to date. To achieve high strain rates $>10^7 \text{ s}^{-1}$, we have adopted a recently developed technique using high-power lasers at the Omega and Janus Laser facilities in Rochester, NY and Livermore, CA, respectively.¹⁰ The electrodeposited nc Ni used in the experiments came from two

sources: (1) Samples with grain sizes in the range of 30–50 nm were purchased from Goodfellow Inc.; and (2) we also electrodeposited Ni samples at several other grain sizes, 30–100 nm.¹¹ The reported grain sizes were measured through extensive plan-view transmission electron microscopy (TEM) examinations of the as-prepared materials. In cross-sectional TEM views, both samples showed slightly elongated grains with an average aspect ratio of about 2.5 (Fig. 1). Such a columnar grain structure is not surprising,^{11,12} in light of the relevant electrodeposition mechanisms and the relatively large thicknesses of the current samples (300 μm).^{5,11,12} The Goodfellow samples were glued to a 3 mm thick Cu substrate for shock-loading experiments.

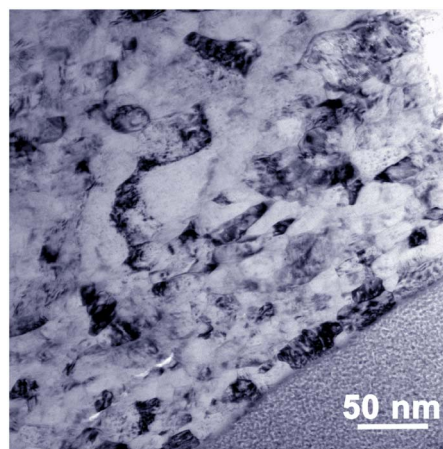


FIG. 1. (Color online) Cross-sectional TEM micrographs of electrodeposited nanocrystalline Ni from Goodfellow, with a grain size of 30–50 nm. There is an elongated grain structure along the thickness direction with an aspect ratio of about 2.5. The amorphous like structure seen in low right corner is the platinum coating applied to protect the surface of TEM samples during FIB processing.

^{a)}Electronic mail: ymwang@llnl.gov

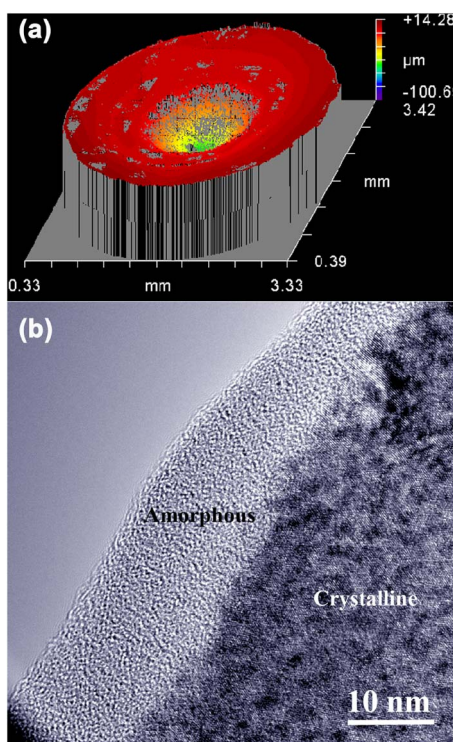


FIG. 2. (Color online) (a) An Ambios white-light profilometry image of the nanocrystalline nickel surface after loading at 20 GPa. (b) Cross-sectional HRTEM image of the amorphous layer at the shock surface of the nc nickel.

The extreme conditions associated with laser-loading generate a complex loading path, which leads to heating, possible surface melting, and extensive plastic deformation, such that a crater is created at the place where the loading is applied. The issue of heating is important for its implications on microstructural stability: Grain growth is known to occur in nc Ni at temperatures as low as 200 °C after 1 h annealing.¹³ Our computational results using hydrodynamic codes¹⁴ indicate that the temperature rise in bulk microcrystalline Ni would be less than 300 K and would only last for a period of a few microseconds, given a shock pressure of 40 GPa. Such a short-time temperature increase is not expected to induce significant grain growth in our shocked samples.

Figure 2(a) illustrates an Ambios white-light profilometry image of a shock crater in nc nickel after a peak loading pressure of ~ 20 GPa; the crater is roughly the size of the laser spot (~ 1 mm²).¹⁴ Near the center of the spot, the loading during the shock is very close to uniaxial, and Hugoniot data predict $\sim 8\%$ strain at 20 GPa and $\sim 13\%$ at 40 GPa. These strains are much larger than those usually supported by nc Ni under uniaxial tensile loading condition.^{4,5}

Shown in Fig. 2(b) is a cross-sectional transmission electron micrograph of an nc Ni sample loaded at ~ 20 GPa, which reveals an unexpected thin layer of amorphous structure on the sample surface. The thickness of this amorphous layer, as measured by high-resolution TEM (HRTEM), is about 10–20 nm. Energy dispersive x-ray spectroscopy analysis indicates that there is a very high oxygen (12 at. %) and carbon (8 at. %) content inside this amorphous layer, likely picked up from a nearby polymer reservoir that is part of the shock-loading system; upon shock, the polymer is released to cross a vacuum gap to the sample surface.¹⁰ These impurities, together with extremely fast cooling rates ($\sim 10^{5-7}$ K/s) after shock loading, apparently caused the

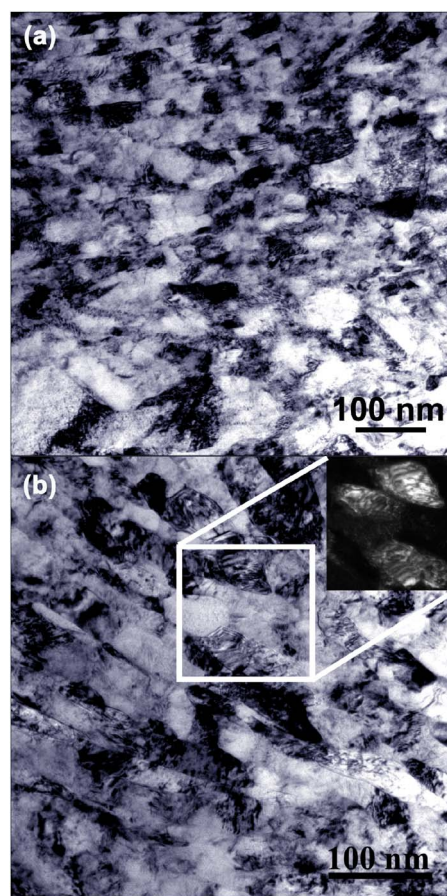


FIG. 3. (Color online) Cross-sectional TEM images of nc nickel after shock loading at (a) 20 GPa, and (b) 40 GPa, showing dislocation activity. The inset in (b) is a dark-field TEM image corresponding to the white square area, in which dislocations are better resolved.

amorphization of nc nickel at the specimen surface. Beneath the thin layer of contaminated, amorphous material, however, our TEM examinations confirmed that the structure remained nanocrystalline.

To precisely locate the uniaxial deformation region of the greatest interest to this work, we used a dual-beam focused ion beam (FIB) to prepare cross-sectional TEM samples from the region 50–150 μm beneath the shock surface, in the center of the original crater. Because FIB processing may induce artifacts into TEM samples,¹⁵ we also prepared some TEM specimens by electropolishing and found no obvious microstructural differences between these two batches of samples. Although there is a small gradient in the applied pressure with depth from the shock surface, no significant differences could be detected in the microstructure to a depth of 150 μm .

Figure 3 shows cross-sectional TEM micrographs of Goodfellow nc Ni samples (initial grain size ~ 30 –50 nm) after shock loading at 20 and 40 GPa, respectively. The TEM samples were taken from the same depth, i.e., 150 μm beneath the shock surface. At both shock pressures, a high density of dislocations was observed, indicating that dislocation generation and motion contribute to plastic deformation in nc nickel under these conditions. No trace of deformation twinning was observed in any of our TEM samples, even for the larger grain sizes of 50–70 nm and a higher shock pressure of ~ 70 GPa. With increasing shock pressures (from 20 to 40 GPa), the dislocation density observed in the deformed

microstructure increased, similarly to the trends seen in shocked microcrystalline samples.^{8,9} Because of significant tangling and overlapping of dislocations, quantitative measurement of the dislocation density in the recovered samples is challenging. From the dark-field images such as the one shown in the inset of Fig. 3(b), the dislocation density is estimated to be $\sim 10^{16} \text{ m}^{-2}$ in the 40 GPa shocked sample. This is remarkably high, considering that quasi-static experiments of nc materials reveal dislocations only during *in situ* straining,^{16,17} and dislocation debris is not typically detected after deformation ceases.¹⁷ The dislocation density found in MD simulations of shocked nc materials⁶ is about one order of magnitude higher than that estimated from the present TEM investigations, which is reasonable given that some dislocations disappear through recovery processes (due to the heat evolution upon loading and stress relaxation upon unloading).¹⁸

Assuming a Hall–Petch-type scaling for the twinning threshold stress,¹⁹ the shock pressure for deformation twinning to occur in nanocrystalline Ni is expected to be higher than 30 GPa.⁹ We did not observe twins up to our highest loading pressure (70 GPa) in any nc Ni sample. This result is somewhat surprising but compares well with MD simulations for 5–200 GPa shock pressures, where abundant dislocations were generated from grain boundaries to accommodate the large shock-induced strains, while deformation twinning was negligible for grain sizes larger than 20 nm.⁶ Our results seem to be in contrast to recent observations of deformation twinning in nc Cu subjected to low strain-rate torsional loading under high pressures,²⁰ although the present experiments access much lower levels of applied shear strain. In more comparable shock experiments on Cu, the twinning threshold is 10–15 GPa for grain sizes $> 100 \mu\text{m}$, but no twins are observed for 9 μm grains at 35 GPa.¹⁸ This is consistent with the trend we have observed here.

We also measured the Vickers hardness of our samples before and after the shocks. The crater surface, where there is melting, contamination with impurities, amorphization, and high-temperature recovery, typically shows a small hardness decrease. Measurements on the cross section, starting 50 μm below the surface, however, show a relative hardness increase of 5–30% after the shock in all cases. This increased hardness is consistent with the stored dislocation density seen in Fig. 3. Since nc metals generally do not work harden under quasi-static loading, shock-induced hardening of nc metals could represent a surface treatment technology with relevance in multiple applications.

In summary, we report unique deformation behavior of nanocrystalline nickel at ultrahigh strain rates ($> 10^7 \text{ s}^{-1}$), achieved through laser-shock-loading experiments (20–70 GPa shock pressures). TEM analysis indicates that the materials remain nc after shock loading, and that dislocation

mechanisms operate at shock pressures of 20–70 GPa and grain sizes above 30 nm. Recent atomistic simulations⁶ showed that nc materials are harder during shock loading, and here, we confirm this prediction through experiment. The increased hardness after shock loading is likely due to the increased dislocation density, as observed in TEM. Additional studies exploring the grain size dependence of shock-induced plasticity are in progress and may offer a more legitimate comparison between experiments and simulations at the same strain rates.

The work at Lawrence Livermore National Laboratory was performed under the auspices of the U. S. Department of Energy by the University of California, Lawrence Livermore National Laboratory under Contract No. W-7405-ENG-48 with support from Laboratory Directed Research and Development Program. The work at MIT was supported by the U.S. Army Research Office. The experimental involvement of B. Y. C. Wu and A. J. Detor (both of MIT) is gratefully recognized.

¹J. Schiøtz and K. W. Jacobsen, *Science* **301**, 1357 (2003).

²V. Yamakov, D. Wolf, S. R. Phillpot, A. K. Mukherjee, and H. Gleiter, *Philos. Mag. Lett.* **83**, 385 (2003).

³H. Van Swygenhoven, P. M. Derlet, and A. G. Frøseth, *Nat. Mater.* **3**, 399 (2004).

⁴D. Jia, K. T. Ramesh, E. Ma, L. Lu, and K. Lu, *Scr. Mater.* **45**, 613 (2001).

⁵F. Dalla Torre, H. Van Swygenhoven, and M. Victoria, *Acta Mater.* **50**, 3957 (2002).

⁶E. M. Bringa, A. Caro, Y. M. Wang, M. Victoria, J. M. McNaney, B. A. Remington, R. F. Smith, B. Torralva, and H. Van Swygenhoven, *Science* **309**, 1838 (2005).

⁷E. V. Esquivel, L. E. Murr, E. A. Trillo, and M. Baquera, *J. Mater. Sci.* **38**, 2223 (2003).

⁸P. S. Follansbee and G. T. Gray, *Int. J. Plast.* **7**, 651 (1991).

⁹F. Greulich and L. E. Murr, *Mater. Sci. Eng.*, **39**, 81 (1979).

¹⁰J. Edwards, K. T. Lorenz, B. A. Remington, S. Pollaine, J. Colvin, D. Braun, B. F. Lasinski, D. Reisman, J. M. McNaney, J. A. Greenough, R. Wallaee, H. Louis, and D. Kalantar, *Phys. Rev. Lett.* **92**, 075002 (2004).

¹¹C. A. Schuh, T. G. Nieh, and T. Yamasaki, *Scr. Mater.* **46**, 735 (2002).

¹²Y. M. Wang, E. Ma, and A. V. Hamza, *Appl. Phys. Lett.* **86**, 241917 (2005).

¹³Y. M. Wang, S. Cheng, Q. M. Wei, E. Ma, T. G. Nieh, and A. V. Hamza, *Scr. Mater.* **51**, 1023 (2004).

¹⁴J. M. McNaney, J. Edwards, R. Becker, T. Lorenz, and B. Remington, *Metall. Mater. Trans. A* **35A**, 2625 (2004).

¹⁵C. Völkert (private communication).

¹⁶K. M. Youssef, R. O. Scattergood, K. L. Murty, J. A. Horton, and C. C. Koch, *Appl. Phys. Lett.* **87**, 091904 (2005).

¹⁷Z. Budrovic, H. Van Swygenhoven, P. M. Derlet, S. Van Petegem, and B. Schmitt, *Science* **304**, 273 (2004).

¹⁸M. A. Meyers, F. Gregori, B. K. Kad, M. S. Schneider, D. H. Kalantar, B. A. Remington, G. Ravichandran, T. Boehly, and J. S. Wark, *Acta Mater.* **51**, 1211 (2003).

¹⁹M. A. Meyers, O. Vöhringer, and V. A. Lubarda, *Acta Mater.* **49**, 4025 (2001).

²⁰X. Z. Liao, Y. H. Zhao, S. G. Srinivasan, Y. T. Zhu, R. Z. Valiev, and D. V. Gunderov, *Appl. Phys. Lett.* **84**, 592 (2004).